Journal of Inorganic and General Chemistry
ZAAC
Zeitschrift für anorganische und allgemeine Chemie
DOI: 10.1002/zaac.201800229
ARTICLE

Synthesis, Structure, and Luminescence Properties of Rare Earth Complexes with β-Diketone containing Imidazole Group

Ping Yang*[a]

Abstract. A series of lanthanide metal complexes [*Ln* = Sm (**1** and **5**), Eu (**2** and **6**), Tb (**3** and **7**), Er (**4** and **8**)] were synthesized with imidazole-containing β-diketone ligands. Complexes **1**–**8** were characterized by IR, elemental analysis, powder XRD, and TG measurements. The photoluminescence properties and the probable mechanism of the Sm, Eu, and Tb complexes were studied. The Eu complex generated strong red light in response to excitation with purple light (380–420 nm). Their fluorescence lifetime of **2** and **6** were 378 and 267 μs, respectively. The measurement and analysis of the thermal properties showed that these were thermal stable. Therefore, it can be applied to LED fluorescent powder.

Introduction

Rare earth ions can generate narrow and high-color purity radiative transitions due to their f-f transition inhibition; furthermore, the emission wavelength rarely changes due to the shielding effect of outer electrons. Therefore, rare earth luminescent materials play a very important role in numerous luminescent materials. The β-diketone rare earth metal complex is a typical representative of rare earth complex luminescent materials[1] and is widely used in many fields.[2] Unfortunately, the absorption of rare earth ions is usually strongest in the ultraviolet region and is weak in the visible region. Excitation with ultraviolet light can easily lead to the destruction of organic ligands, thus restricting their application. Therefore, to solve this problem, the excitation light must be moved into the visible region.

Generally, two types of strategies are applied to achieve this: Firstly, 4d or 5d transition metal ions are introduced and transition metal parts are utilized with stronger absorption in the visible region and an energy level charge transition (^{3}MLCT) close to that of rare earth ions. This enables the visible light to excite transition metal chromophore sensitized rare earth to emit light, thus increasing the applicability of the materials.[3] For example, *Huang* et al. synthesized a tetranuclear Ir_3Eu complex via connecting a β-diketone group to phenanthroline, which can emit strong red light under an excitation of 530 nm.[4] Secondly, a stable large π-conjugated system is employed to modify β-diketone ligand, thus moving the exciting light into the visible region via red shift. For example, *Gong* et al. prepared a ternary Eu complex using β-diketone ligand modified with carbazole, which can generate strong red light in response to excitation with blue light of 460 nm.[5]

* Dr. P. Yang
E-Mail: 191723030@qq.com
[a] School of Environment
Jinan University
Guangzhou 511443, P. R. China
Supporting information for this article is available on the WWW under **http://dx.doi.org/10.1002/zaac.201800229** or from the author.

β-Diketone and rare earth ions possess good coordination capabilities and luminescence properties,[2c,6] however, studies on heterocyclic N-ring β-diketone rare earth complexes mainly focused on carbazole[1b,5,7] 4-acylpyrazolone,[8] and pyridine,[9] and rarely used imidazole.[10] Therefore, in this study, we choose a stable large π-conjugated system ligand 1-(4-(1*H*-imidazol-yl)phenyl)butane-1,3-dione to construct a series of rare earth complexes, and study the relationship between the structures and photoluminescence properties.

Results and Discussion

Crystal Structure

Table 1 shows that complexes **1**–**4** all belong to monoclinic space group *Cc* and cell parameters *a*, *b*, *c*, and *V* decreased in turn, which is in line with the contraction law of lanthanide series metal ions. For the sake of brevity, only complex **2** is chosen as the representative for structural description. The asymmetric unit contains one Eu^{III} ion, three $IPBD^-$ molecules, one coordinated water molecule, and two lattice solvent molecules (H_2O and DMF). Each Eu^{III} ion shows an eight coordination mode and is surrounded by six O atoms from three ligands, one O atom from a water molecule, and one imidazole N atom, forming a square antiprism arrangement (Figure 1a and Figure 1b). The bond length of $Eu–O_{dionate}$ is in the range of 2.333(6)–2.427(6) Å, whereas that of $Eu–O_{water}$ is slightly longer with 2.486(6) Å, and that of Eu–N is 2.605(6) Å. The ligands have two types of coordination modes. Among them, two ligands adopt the bidentate mode and the third ligand adopts a tridentate bridge mode, linking neighboring Eu^{III} ions and forming one-dimensional chains (Figure 1c). Similar to the reported structure of $[Eu(4\text{-}PBD)_3(H_2O)]$,[9] they have two uncoordinated N atoms on the outside of the chains. Each chain is linked to the neighboring four chains through a O1w–H1w···N3 (2.842 Å, 144.62°) hydrogen-bond interaction and form a three-dimensional structure.

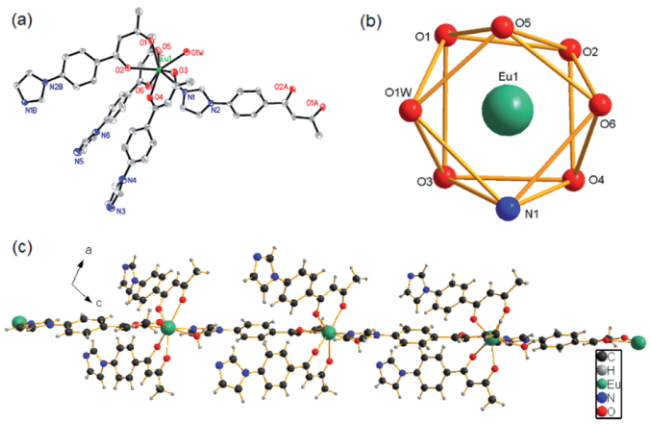

Figure 1. ORTEP drawing with thermal ellipsoids at 30 % probability, coordination sphere around Eu^{III} and 1D chain along the *b* axis of complex **2**; symmetry code: A: 1/2 + *x*, 1/2 –*y*, 1/2 + *z*; B: –1/2 + *x*, 1/2 –*y*, –1/2 + *z*.

Table 2 shows that complexes **5**–**8** all belong to monoclinic space group $P2_1/c$ and the cell parameters *a*, *b*, *c*, and *V* decrease in turn, which is in line with the contraction law of lanthanide series metal ions. Therefore, complex **6** was used as example for the discussion. The asymmetric unit contains one Eu^{III} ion, three $IPBD^-$ molecules, and one lattice water molecule. Each Eu^{III} ion shows an eight coordination mode and is surrounded by six O atoms from three ligands and two imidazole N atoms from the remaining two ligands, forming a square antiprism arrangement (Figure 2a and Figure 2b). The bond length of Eu–$O_{dionate}$ is in the range of 2.310(2)–2.416(2) Å, and that of Eu–N is 2.606(2)–2.614(2) Å. The ligands have two types of coordination modes. Among them, one ligand adopts the bidentate mode, whereas the other two adopt tridentate bridge mode. Compared to complex **2**, where a coordinated water molecule of Eu^{III} ion is replaced by the imidazole N atom, the dimension increases to two-dimensional and the topological type is **sql** tetragonal plane net ($4^4;6^2$)

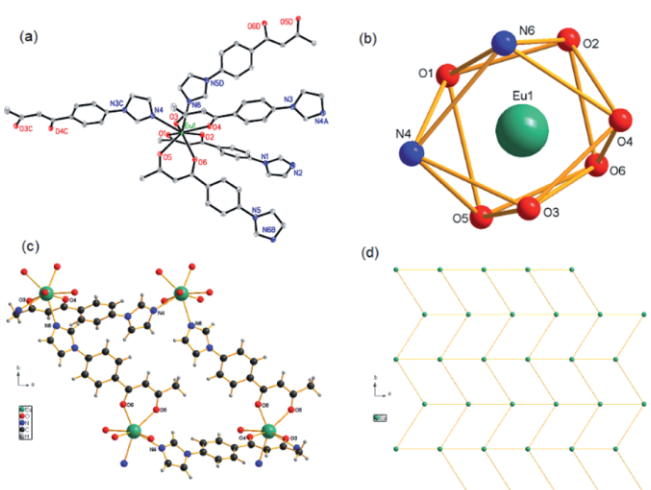

Figure 2. ORTEP drawing with thermal ellipsoids at 30 % probability, coordination sphere around Eu^{III}, 2D layer along the *c* axis and schematic drawing of complex **6**; symmetry code: A: –1+x, *y*, *z*; B: 1 –*x*, 1/2 + *y*, 1/2 –*z*; C: 1+x, *y*, *z*; D: 1 –*x*, –1/2 + *y*, 1/2 –*z*.

(Figure 2c and Figure 2d). All layers present an interleaving stack of AB···pattern (Figure 3).

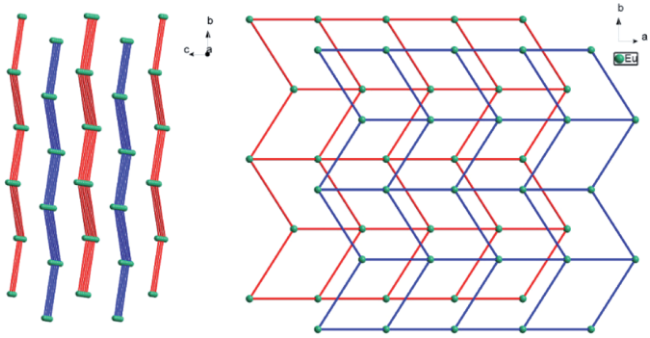

Figure 3. Stacked diagram of complex **6**.

Powder X-ray Diffraction

The purity of the bulky products of the complexes was confirmed by elemental analysis (see Experimental Section). The phase purity of the bulky sample is measured by powder X-ray diffraction. The experimental and simulated XRD patterns of **1**–**8** are shown in Figure S1 and Figure S2 (Supporting Information). The powder X-ray diffraction patterns of complexes **1**–**8** agreed very well with the powder X-ray diffraction patterns simulated according to their X-ray single-crystal data, thus indicating that the products were pure phase. The pure crystalline samples are thus suitable for studies of photoluminescent properties.

Thermal Analysis

The thermogravimetric (TG) analysis experiments were performed to determine the thermal stability of the complex **2** and **6**. As shown in Figure S3 (Supporting Information), complex **2** underwent a weight loss of 9.33 % at about 160 °C, corresponding to one lattice H_2O molecule and one DMF molecule (calcd. 9.65 %). The weight loss of 12.03 % at 180 °C corresponded to one coordination H_2O molecule (calculated 11.56 %). There was a phase change at around 235 °C and the overall stability was around 300 °C. The TG curve in Figure S4 (Supporting Information) indicates that complex **6** gradually underwent a weight loss of 3.00 % before 50 °C, corresponding to one lattice water molecule (calculated 2.11 %). Overall, it can keep stable at about 250 °C.

Luminescent Properties

Figure 4 shows that under excitation of 367 nm, the strongest emission peak of complex **1** could be found in the red light of 649 nm ($^4G_{5/2}\rightarrow{}^6H_{9/2}$), not in the common light of 595 nm ($^4G_{5/2}\rightarrow{}^6H_{7/2}$). The symmetry around the Sm^{III} ion was low, which was conducive to electric dipole transition.[11] Under excitation of 389 nm, the strongest emission peak of complex **2** was in the red light of 612 nm ($^5D_0\rightarrow{}^7F_2$) and could be divided into three peaks. The coordination environment occupied

by the Eu^{III} ion in the complex was D_2 symmetrical, but the X-ray single-crystal data shows a C_s symmetry (Figure 1b), which may be that the split is incomplete at room temperature.

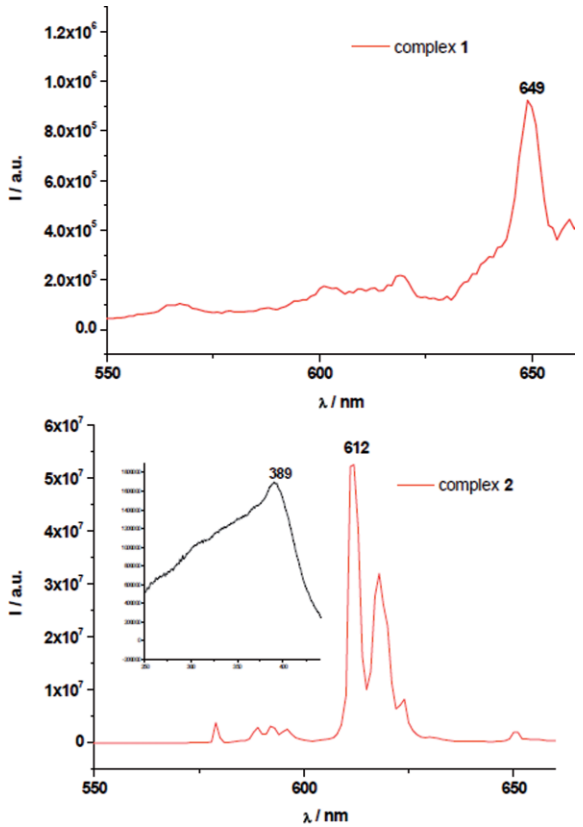

Figure 4. Fluorescence spectra of complexes **1** (λ_{ex} = 367 nm) and **2** (λ_{ex} = 389 nm).

The CIE chromaticity coordinate (0.666, 0.3332) was very close to NTSC standard (0.67, 0.33). However, complex **3** did not emit luminescence. Thus, it can be learned that the triplet state energy of ligand HIPBD was close to or lower than the $^5D_4$ energy of Tb^{III} ion (20400 cm^{-1}) because the optimal luminescence energy-level difference was 2500–3500 cm^{-1}[12] even the lowest requirement should exceed 1850 cm^{-1}.[13] This can also be seen from the ligand's ultraviolet spectrum and fluorescence spectrum of the ligand (Figure S5, Supporting Information). The maximum absorption of ligand HIPBD was at 320 nm ($\varepsilon = 4.63 \times 10^4$ L·mol^{-1}·cm^{-1}) and had strong light absorption capability. The S_1 excitation state energy was 27027 cm^{-1} (370 nm, estimated according to the margin of ultraviolet absorption peak[14]), followed by a non-radiative transition to the T_1 state (20833 cm^{-1}, 480 nm), which conforms to the optimal energy difference (≈ 5000 cm^{-1}).[12,15] The triplet energy was comparable to that of 1-(4-(1H-imidazol-1-yl)phenyl)-4,4,4-trifluoro-1,3-butanedione reported in the literature (18416 cm^{-1}, 543 nm).[10] The possible luminous mechanisms are shown in Figure 5. Measuring the attenuation curve of Eu^{III} ion $^5D_0 \rightarrow {}^7F_2$ (612 nm), complex **2** has two fluorescence lifetimes: 207 μs (6%) and 378 μs (94%) (Figure S6, Supporting Information).

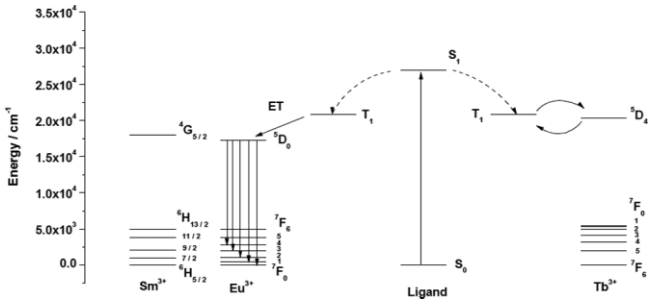

Figure 5. Luminous mechanism graph of complex **2**.

Figure 6 shows that under excitation of 367 nm, the strongest emission peak of complex **5** was in the red light of 650 nm ($^4G_{5/2} \rightarrow {}^6H_{9/2}$), while it was weaker in the light of 561 nm ($^4G_{5/2} \rightarrow {}^6H_{5/2}$) and 595 nm ($^4G_{5/2} \rightarrow {}^6H_{7/2}$). Moreover, the fluorescence intensity was stronger than that of complex **1**. The symmetry around the Sm^{III} ion was lower than that of complex **1**, which was favorable for electric dipole transition. Under the excitation of 397 nm, the strongest emission peak of complex **6** could be found in the red light of 612 nm ($^5D_0 \rightarrow {}^7F_2$), and it could be divided into five peaks. It is well-known that the strongest $^5D_0 \rightarrow {}^7F_2$ transition is sensitive to the coordination environment around the central Eu^{III} atom and could be increased along with a symmetric decrease in the central ion.[16] The coordination environment occupied by the Eu^{III} ion in the complex was C_s, C_2, or C_1 symmetry, which

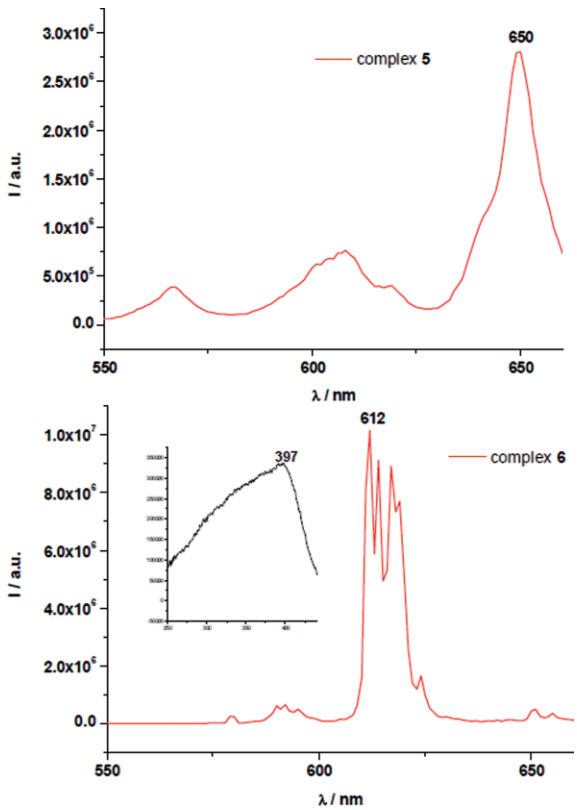

Figure 6. Fluorescence spectra of complexes **5** (λ_{ex} = 367 nm) and **6** (λ_{ex} = 397 nm).

was C_s symmetry derived from the result of X-ray single-crystal data (Figure 2b).

The CIE chromaticity coordinate (0.663, 0.328) was very close to the NTSC standard (0.67, 0.33). Generally, Tb^{III} can emit green-light through the transitions of $^5D_4 \rightarrow {}^7F_J$ (J = 6, 5, 4, and 3)[17]. However, complex **7** did not generate luminescence. It can be seen that the triplet energy of the ligand HIPBD was close to or lower than the $^5D_4$ energy (20400 cm^{-1}) of the Tb^{III} ion since the optimum emission energy level difference was 2500–3500 cm^{-1}[12]. This can also be seen from the ligand's ultraviolet spectrum and fluorescence spectrum of the ligand (Figure S5, Supporting Information). The analysis yielded the same result as above. Figure S7 (Supporting Information) shows that complex **6** has two fluorescence lifetimes: 162 μs (18 %) and 267 μs (82 %). Considering its excitation wavelength and thermal stability, it can be applied to LED fluorescent powder.

Conclusions

In this study, ligand HIPBD was used to cultivate eight complexes of two categories via room temperature volatilization and solvothermal methods. Among them, complexes **1**–**4** have a one-dimensional chain structure, whereas complexes **5**–**8** have a two-dimensional **sql** layer structure. Increasing temperature and pressure can increase the structure's dimension. In the near ultraviolet region, ligand HIPBD has a strong light absorption capability. The introduction of imidazole groups increases the electron density and allowed the red light of the complex to move into the visible region. Under violet excitation, complexes **2** and **6** can emit strong red light. Complex **6** has no coordination solvent and high thermal stability, which indicated them as a potential LED fluorescent powder material.

Experimental Section

Materials and Physical Methods: The reagents and solvents used in this study are all of analytical purity and have not been pre-processed prior to use. Elemental analysis (C, H, and N) was conducted with an Elementar Vario EL elemental analyzer. IR spectra were measured with a Bruker TENSOR 27 (4000–400 cm^{-1}) FT-IR spectrometer using KBr pellets. Thermal analysis was conducted with a Netzsch TG 209 F3 Tarsus thermogravimetric analyzer (nitrogen atmosphere). The reference compound was Al_2O_3 and the heating rate was 10 K·min^{-1}. Powder X-ray diffraction (PXRD) was tested with a Bruker D8 advance diffractiometer, with Cu-K_α radiation (λ = 0.15409 nm) at 4° per min and a scanning angle of 5–35°. The powder X-ray diffraction pattern, simulated with single-crystal structure, was generated by the software Mercury 1.4.2. Fluorescence spectra were collected with an EDINBURGH FLSP920. The ligand 1-(4-(1*H*-imidazol-yl)phenyl)butane-1,3-dione (HIPBD) was synthesized by our previous articles[18].

Synthesis of Complexes 1–4: A solution of $SmCl_3$ (0.03 mmol) in methanol (0.5 mL) was added dropwise to a solution of HIPBD (0.1 mmol) and $N(Et)_3$ (14 μL) in ethanol (3 mL). The solution was slightly turbid after shaking. Subsequently, DMF (0.5 mL) was added and the solution became clear. After one week of static evaporation, pink crystals $[Sm(IPBD)_3(H_2O)]\cdot DMF\cdot H_2O$ (**1**) were obtained (yield 85 % based on Sm). $C_{42}H_{44}N_7O_9Sm$: calcd. C 53.55; H 4.67; N 10.41 %; found: C 53.54; H 4.66; N 10.43 %. **IR** (KBr): $\tilde{\nu}$ = 3398 w, 3123 w, 1655 s, 1595 s, 1571 s, 1508 s, 1449 s, 1404 s, 1303 s, 1266 m, 1195 w, 1118 w, 1104 w, 1059 m, 1016 w, 999 w, 963 m, 845 m, 770 m, 697 w, 657 w, 566 w, 417 w cm^{-1}.

After replacing $SmCl_3$ with $EuCl_3$, a clear crystal $[Eu(IPBD)_3(H_2O)]\cdot DMF\cdot H_2O$ (**2**) was obtained (yield 85 % based on Eu). $C_{42}H_{44}N_7O_9Eu$: calcd. C 53.46; H 4.67; N 10.39 %; found: C 53.46; H 4.65; N 10.40 %. **IR** (KBr): $\tilde{\nu}$ = 3413 w, 3123 w, 1655 m, 1596 s, 1570 s, 1500 s, 1448 s, 1401 s, 1303 s, 1264 m, 1199 w, 1118 w, 1058 m, 1016 w, 999 w, 963 m, 846 m, 771 m, 698 w, 657 w, 566 w, 418 w cm^{-1}.

After replacing $SmCl_3$ with $TbCl_3$, a clear crystal $[Tb(IPBD)_3(H_2O)]\cdot DMF\cdot H_2O$ (**3**) was obtained (yield 85 % based on Tb). $C_{42}H_{44}N_7O_9Tb$: calcd. C 53.07; H 4.63; N 10.32 %; found: C 53.05; H 4.65; N 10.33 %. **IR** (KBr): $\tilde{\nu}$ = 3390 w, 3122 w, 1656 s, 1600 s, 1571 s, 1505 s, 1449 s, 1402 s, 1303 s, 1266 m, 1195 w, 1118 w, 1104 w, 1059 m, 1015 w, 999 w, 963 m, 846 m, 770 m, 697 w, 656 w, 568 w, 418 w cm^{-1}.

After replacing $SmCl_3$ with $ErCl_3$, a pink crystal $[Er(IPBD)_3(H_2O)]\cdot DMF\cdot H_2O$ (**4**) was obtained (yield 85 % based on Er). $C_{42}H_{44}N_7O_9Er$: calcd. C 52.60; H 4.59; N 10.23 %; found: C 52.61; H 4.58; N 10.23 %. **IR** (KBr): $\tilde{\nu}$ = 3397 w, 3122 w, 1657 m, 1596 s, 1571 s, 1504 s, 1454 s, 1405 s, 1303 s, 1266 m, 1195 w, 1118 w, 1103 w, 1059 m, 999 w, 962 w, 847 m, 770 m, 698 w, 657 w, 570 w, 422 w cm^{-1}.

Synthesis of Complexes 5–8: $N(Et)_3$ (42 μL) and $SmCl_3$ (0.1 mmol) were added to a solution of HIPBD (0.3 mmol) in acetonitrile (4 mL). After shaking, the mixture was placed into a 23 mL Teflon-lined stainless steel reactor and was heated to 130 °C for 72 h. After it had cooled to room temperature at 5 K·h^{-1}, clear crystals $[Sm(IPBD)_3]\cdot H_2O$ (**5**) were obtained (yield 45 % based on Sm). $C_{39}H_{35}N_6O_7Sm$: calcd. C, 55.05; H 4.12; N 9.88 %; found: C 55.06; H 4.11; N 9.89 %. **IR** (KBr): $\tilde{\nu}$ = 3405 w, 3137 w, 1596 s, 1569 s, 1504 s, 1453 s, 1405 s, 1303 s, 1278 m, 1259 m, 1245 m, 1205 w, 1185 w, 1118 w, 1056 m, 1016 w, 995 w, 963 m, 923 w, 844 m, 773 m, 735 w, 697 w, 656 w, 565 w, 418 w cm^{-1}.

After replacing $SmCl_3$ with $EuCl_3$, a clear crystal $[Eu(IPBD)_3]\cdot H_2O$ (**6**) was obtained (yield 45 % based on Eu). $C_{39}H_{35}N_6O_7Eu$: calcd. C 54.95; H 4.11; N 9.86 %; found: C 54.94; H 4.12; N 9.87 %. **IR** (KBr): $\tilde{\nu}$ = 3412 w, 3138 w, 1597 s, 1569 s, 1505 s, 1453 s, 1405 s, 1303 s, 1279 w, 1259 w, 1245 w, 1205 w, 1185 w, 1118 w, 1055 m, 1016 w, 995 w, 963 m, 923 w, 844 m, 773 m, 735 w, 696 w, 656 w, 565 w, 418 w cm^{-1}.

After replacing $SmCl_3$ with $TbCl_3$, a clear crystal $[Tb(IPBD)_3]\cdot H_2O$ (**7**) was obtained (yield 45 % based on Tb). $C_{39}H_{35}N_6O_7Tb$: calcd. C, 54.50; H 4.08; N 9.78 %; found: C 54.52; H 4.06; N 9.77 %. **IR** (KBr): $\tilde{\nu}$ = 3401 w, 3139 w, 1597 s, 1569 s, 1507 s, 1454 s, 1406 s, 1303 s, 1280 w, 1259 w, 1245 w, 1206 w, 1186 w, 1118 w, 1056 m, 1016 w, 996 w, 963 m, 924 w, 844 m, 773 m, 735 w, 697 w, 656 w, 567 w, 418 w cm^{-1}.

After replacing $SmCl_3$ with $ErCl_3$, a clear crystal $[Er(IPBD)_3]\cdot 0.5H_2O$ (**8**) was obtained (yield 45 % based on Er). $C_{39}H_{35}N_6O_7Er$: calcd. C, 54.55; H 3.96; N 9.79 %; found: C 54.54; H 3.96; N 9.82 %. **IR** (KBr): $\tilde{\nu}$ = 3426 w, 3143 w, 1598 s, 1570 s, 1506 s, 1457 s, 1404 s, 1303 s, 1282 w, 1260 w, 1246 w, 1205 w, 1186 w, 1118 w, 1056 m, 1016 w, 999 w, 963 w, 846 w, 773 m, 734 w, 698 w, 657 w, 568 w, 420 w cm^{-1}.

X-ray Crystallography: Data for the complexes of **1–8** was performed with a Bruker Smart Apex CCD area detector and Rigaku R-AXIS SPIDER IP to collect the diffraction data (Mo-K_α, λ = 0.071073 nm), and the SADABS program was used for absorption correction. The crystal structure was solved directly through the direct method and then, the SHELXTL program package was used to conduct full-matrix least square structure refinement based on F^2. Except for extremely severely disordered atoms, other non-hydrogen atoms were all anisotropically refined. The geometric hydrogenation method was used to add hydrogen atoms on the organic group and the differential Fourier synthesis method was used to add hydrogen atoms on solvent water. Further details of the X-ray structural analyses for complexes **1–8** are given in Table 1 and Table 2. The selected bond lengths for **1–8** are listed in Table S1 and Table S2 (see Supporting Information).

Crystallographic data (excluding structure factors) for the structures in this paper have been deposited with the Cambridge Crystallographic Data Centre, CCDC, 12 Union Road, Cambridge CB21EZ, UK. Copies of the data can be obtained free of charge on quoting the depository numbers CCDC-827343, CCDC-827341, CCDC-827345, CCDC-827339, CCDC-827342, CCDC-827340, CCDC-827344, and CCDC-827338 for **1–8** (Fax: +44-1223-336-033; E-Mail: deposit@ccdc.cam.ac.uk, http://www.ccdc.cam.ac.uk).

Supporting Information (see footnote on the first page of this article): PXRD patterns, TG curve, UV spectra, luminescence decay curves, selected bond lengths of **1–8** or HIPBD.

Table 1. Crystal data and structure refinement for complexes **1–4**.

	1	**2**	**3**	**4**
Empirical formula	$C_{42}H_{44}N_7O_9Sm$	$C_{42}H_{44}N_7O_9Eu$	$C_{42}H_{44}N_7O_9Tb$	$C_{42}H_{44}N_7O_9Er$
Formula weight	941.19	942.80	949.76	958.10
Temperature /K	298(2)	298(2)	293(2)	293(2)
Wavelength /Å	0.71073	0.71073	0.71073	0.71073
Crystal system	monoclinic	monoclinic	monoclinic	monoclinic
Space group	*Cc*	*Cc*	*Cc*	*Cc*
a /Å	16.9018(6)	16.8726(7)	16.8674(6)	16.8291(17)
b /Å	11.0250(4)	11.0221(4)	11.0112(4)	10.9859(13)
c /Å	23.7160(9)	23.6802(10)	23.6467(8)	23.515(3)
β /°	109.2610(10)	109.3275(11)	109.3870(10)	109.479(3)
V /Å^3	4171.9(3)	4155.6(3)	4142.9(3)	4098.7(8)
Z	4	4	4	4
D_c /Mg·m^{-3}	1.498	1.507	1.523	1.553
μ /mm^{-1}	1.471	1.573	1.771	2.112
F(000)	1916	1920	1928	1940
Reflections collected	10987	10717	12263	21274
Unique, R_{int}	6901, 0.0376	6580, 0.0371	6648, 0.0243	8977, 0.0290
Data/restraints/parameters	6901 / 5 / 537	6580 / 2 / 537	6648 / 5 / 537	8977 / 8 / 537
GOF on F^2	1.065	1.107	1.120	1.176
R_1 [$I > 2\sigma(I)$]	0.0301	0.0380	0.0234	0.0271
wR_2 (all data)	0.0714	0.1299	0.0734	0.0850
Flack parameter	–0.009(10)	–0.033(19)	–0.027(10)	0.030(9)
$\Delta\rho_{max}$ / $\Delta\rho_{min}$ /e·Å^{-3}	1.002 / –0.551	1.259 / –1.083	0.779 / –0.574	0.668 / –0.497

Table 2. Crystal data and structure refinement of complexes **5–8**.

	5	**6**	**7**	**8**
Empirical formula	$C_{39}H_{35}N_6O_7Sm$	$C_{39}H_{35}N_6O_7Eu$	$C_{39}H_{35}N_6O_7Tb$	$C_{78}H_{68}N_{12}O_{13}Er_2$
Formula weight	850.08	851.69	858.65	1715.96
Temperature /K	123(2)	123(2)	123(2)	298(2)
Wavelength /Å	0.71073	0.71073	0.71073	0.71073
Crystal system	monoclinic	monoclinic	monoclinic	monoclinic
Space group	$P2_1/c$	$P2_1/c$	$P2_1/c$	$P2_1/c$
a /Å	12.8225(6)	12.8020(6)	12.7648(6)	12.7368(3)
b /Å	21.1944(10)	21.1912(10)	21.1420(10)	21.3148(6)
c /Å	16.5207(6)	16.5023(6)	16.4780(6)	16.5643(3)
β /°	125.941(2)	125.796(2)	125.551(2)	124.8130(10)
V /Å^3	3635.0(3)	3631.2(3)	3618.0(3)	3692.05(15)
Z	4	4	4	2
D_c /Mg·m^{-3}	1.553	1.558	1.576	1.544
μ /mm^{-1}	1.674	1.786	2.014	2.329
F(000)	1716	1720	1728	1720
Reflections collected	23722	19712	21054	24245
Unique, R_{int}	7132, 0.0282	7108, 0.0228	7080, 0.0245	7105, 0.0409
Data/restraints/parameters	7132 / 3 / 481	7108 / 0 / 481	7080 / 0 / 481	7105 / 3 / 478
GOF on F^2	1.052	1.034	1.041	1.025
R_1 [$I > 2\sigma(I)$]	0.0290	0.0310	0.0295	0.0302
wR_2 (all data)	0.0706	0.0849	0.0752	0.0722
Flack parameter	1.358 / –0.674	2.074 / –0.680	1.647 / –0.575	0.661 / –0.839

Acknowledgements

This work was supported by the National Natural Science Foundation of China (Grant 41701349) and Sun Yat-Sen University.

Keywords: Imidazole-containing β-diketone; Rare earths; Luminescence; Fluorescence lifetime

References

[1] a) A. P. Bassett, S. W. Magennis, P. B. Glover, D. J. Lewis, N. Spencer, S. Parsons, R. M. Williams, L. De Cola, Z. Pikramenou, *J. Am. Chem. Soc.* **2004**, *126*, 9413–9424; b) Z.-J. Hu, X.-H. Tian, X.-H. Zhao, P. Wang, Q. Zhang, P.-P. Sun, J.-Y. Wu, J.-X. Yang, Y.-P. Tian, *Chem. Commun.* **2011**, *47*, 12467–12469; c) S. Swavey, J. A. Krause, D. Collins, D. D′Cunha, A. Fratini, *Polyhedron* **2008**, *27*, 1061–1069; d) M. Fernandes, V. de Zea Bermudez, R. A. Sá Ferreira, L. D. Carlos, A. Charas, J. Morgado, M. M. Silva, M. J. Smith, *Chem. Mater.* **2007**, *19*, 3892–3901; e) S. Gago, J. A. Fernandes, J. P. Rainho, R. A. Sá Ferreira, M. Pillinger, A. A. Valente, T. M. Santos, L. D. Carlos, P. J. A. Ribeiro-Claro, I. S. Gonçalves, *Chem. Mater.* **2005**, *17*, 5077–5084; f) X.-Y. Chen, X. Yang, B. J. Holliday, *J. Am. Chem. Soc.* **2008**, *130*, 1546–1547.

[2] a) P. A. Vigato, V. Peruzzo, S. Tamburini, *Coord. Chem. Rev.* **2009**, *253*, 1099–1201; b) H. Tsukube, S. Shinoda, *Chem. Rev.* **2002**, *102*, 2389–2404; c) J. Kido, Y. Okamoto, *Chem. Rev.* **2002**, *102*, 2357–2368.

[3] H.-B. Xu, Z.-N. Chen, *Chin. J. Inorg. Chem.* **2011**, *27*, 1887–1903.

[4] F.-F. Chen, Z.-Q. Bian, Z.-W. Liu, D.-B. Nie, Z.-Q. Chen, C.-H. Huang, *Inorg. Chem.* **2008**, *47*, 2507–2513.

[5] a) P. He, H. H. Wang, H. G. Yan, W. Hu, J. X. Shi, M. L. Gong, *Dalton Trans.* **2010**, *39*, 8919–8924; b) P. He, H. H. Wang, S. G. Liu, J. X. Shi, G. Wang, M. L. Gong, *Inorg. Chem.* **2009**, *48*, 11382–11387.

[6] a) A. de Bettencourt-Dias, *Dalton Trans.* **2007**, 2229–2241; b) K. Binnemans, J. C. B. K. A. Gschneidner, V. K. Pecharsky, in *Handbook on the Physics and Chemistry of Rare Earths*, vol. 35, Elsevier, **2005**, pp. 107–272.

[7] M. R. Robinson, M. B. O'Regan, G. C. Bazan, *Chem. Commun.* **2000**, 1645–1646.

[8] a) H. Xin, M. Shi, X. C. Gao, Y. Y. Huang, Z. L. Gong, D. B. Nie, H. Cao, Z. Q. Bian, F. Y. Li, C. H. Huang, *J. Phys. Chem. B* **2004**, *108*, 10796–10800; b) H. Xin, F. Y. Li, M. Shi, Z. Q. Bian, C. H. Huang, *J. Am. Chem. Soc.* **2003**, *125*, 7166–7167; c) L. Shen, M. Shi, F. Li, D. Zhang, X. Li, E. Shi, T. Yi, Y. Du, C. Huang, *Inorg. Chem.* **2006**, *45*, 6188–6197; d) S. Capecchi, O. Renault, D. G. Moon, M. Halim, M. Etchells, P. J. Dobson, O. V. Salata, V. Christou, *Adv. Mater.* **2000**, *12*, 1591–1594.

[9] F. Liu, Y. Zhou, *Inorg. Chem. Commun.* **2010**, *13*, 1410–1413.

[10] H. Wang, P. He, H. Yan, J. Shi, M. Gong, *Inorg. Chem. Commun.* **2011**, *14*, 1183–1185.

[11] Y. Hasegawa, S.-i. Tsuruoka, T. Yoshida, H. Kawai, T. Kawai, *J. Phys. Chem. A* **2008**, *112*, 803–807.

[12] J.-C. G. Bünzli, S. V. Eliseeva, in *Lanthanide Luminescence*, vol. 7 (Eds.: P. Hänninen, H. Härmä), Springer Berlin Heidelberg, **2011**, pp. 1–45.

[13] M. Latva, H. Takalo, V.-M. Mukkala, C. Matachescu, J. C. Rodríguez-Ubis, J. Kankare, *J. Lumin.* **1997**, *75*, 149–169.

[14] M. Shi, F. Li, T. Yi, D. Zhang, H. Hu, C. Huang, *Inorg. Chem.* **2005**, *44*, 8929–8936.

[15] F. J. Steemers, W. Verboom, D. N. Reinhoudt, E. B. van der Tol, J. W. Verhoeven, *J. Am. Chem. Soc.* **1995**, *117*, 9408–9414.

[16] a) D. Peng, L. Yin, P. Hu, B. Li, Z.-W. Ouyang, G.-L. Zhuang, Z. Wang, *Inorg. Chem.* **2018**, *57*, 2577–2583; b) W.-X. Chen, J.-q. Bai, Z.-h. Yu, Q.-p. Liu, G.-n. Zeng, G.-l. Zhuang, *Inorg. Chem. Commun.* **2015**, *60*, 4–7.

[17] J. Dong, H. Xu, S.-L. Hou, Z.-L. Wu, B. Zhao, *Inorg. Chem.* **2017**, *56*, 6244–6250.

[18] a) P. Yang, H.-Y. Zhou, K. Zhang, B.-H. Ye, *CrystEngComm* **2011**, *13*, 5658–5660; b) P. Yang, J.-J. Wu, H.-Y. Zhou, B.-H. Ye, *Cryst. Growth Des.* **2012**, *12*, 99–108.

Received: June 2, 2018
Published online: July 13, 2018

